

## Receiver statics correction of *PS*-wave using prestack data in the receiver domain

Saul E. Guevara, and Gary F. Margrave\*

### ABSTRACT

It is proposed a receiver statics correction method for the converted wave data (*PS*-wave). The method is based on the observation that the static time delay on *PS*-wave events between two adjacent receivers, after application of the source statics correction, should correspond mostly to the differential receiver statics. The method does not require stack or a velocity model for *PS*-waves. It follows the surface consistent statics theory applied to Common Receiver Gathers (CRG). Crosscorrelations of the corresponding traces after minimizing the NMO differential and assuming small structural component, are calculated and then stacked. The differential statics time delay should correspond to the maximum of this stack. Tests on synthetic data show encouraging results.

### INTRODUCTION

The statics correction aims to overcome the delay caused by the near surface layer (NSL) on seismic waves reflected at deeper layers. Since *S*-waves propagate more slowly and are not affected by the water table, it makes statics correction more critical and difficult to obtain on them compared to *P*-waves.

In the case of converted wave (*PS*-wave) *S*-waves corresponds to the receiver statics correction, for which several methods have been proposed. Two approaches can be identified (Cox, 1999): methods that require a NSL velocity model (or *datum statics*) and methods based on the surface consistent model, such as the one applied to *PP* residual statics (e.g. Cox, 1999; Taner et al., 1974), focused on the receiver statics correction.

The methods based on the NSL velocity model have shown lower accuracy (and perhaps lower resolution) than required (e.g. Schafer, 1993), which can be attributed to difficulties in event picking (e.g. AlDulaijan, 2008) or even to their physical principles. The methods based on the surface consistent model (e.g. Harrison, 1992; Cary and Eaton, 1992) appear more effective, which can be related to their capability for short wavelength statics resolution. However its calculation frequently is cumbersome and laborious. Besides that they require *PS*-wave reflections, that is to say a model for stacking and an approximate model of the velocity ( $V_c$ ), which is not always good enough.

On the other hand, the NSL *S*-wave velocity model (see Guevara et al., 2013) can present issues to take into account, such as: the shallower near surface (less than about 15 m depth in Guevara et al., 2013) appears as the most influential, since its velocity can be less than 200 m/s, consequently the *S*-wave time delay can be quite significant, and it is not easy to obtain such a low velocity model with refraction or surface wave methods, since it would require close surface sampling. These are additional challenges for the datum statics

---

\*CREWES / Univ. of Calgary

methods.

An alternative approach to obtain a statics correction of the receiver for  $PS$  data is proposed in the following. It can allow a short wavelength solution, since is based on the surface consistent model, but without the requirement of the  $PS$ -wave stack. It is carried out on surface receiver gathers using data without NMO correction, founded on the principle that all the  $PS$ -wave events of a common receiver gather are affected by the same  $S$ -wave static. That is to say, instead of being based in a depth domain such as the CCP (Common Conversion Point), it is a technique based on a surface domain. Techniques for conventional seismic data statics using prestack data in the surface domains Common Receiver Gather (or CRG and Common Shot Gather (or CSG) are presented by Disher and Naquin (1970) and Cox (1999). The method principles and a test with synthetic data are presented in the following sections.

## THEORY

The alternative approach proposed is based on the principle that all the  $PS$ -wave events of a common receiver gather are affected by the same  $S$ -wave statics, according to the surface consistent model, which is described by the next equation (Taner et al., 1974):

$$T_{ijk} = R_i + S_j + G_k + M_k h_{ij}^2 \quad (1)$$

where  $R_i$  = receiver statics at the  $i_t h$  receiver position.  $S_j$  = Source statics at  $j_t h$  source position.  $G_k$  = arbitrary time shift for  $k$ th CDP gather.  $M_k$  = residual NMO component at  $k$ th CDP gather, and  $h_{ij}$  = source to receiver distance (Taner et al., 1974, uses  $(j - i)$  instead.)

Then, in principle, it would be possible to obtain the differential delay time between receivers from the delay time of each trace with the corresponding trace of the adjacent receiver. Thus it would be required to use traces organized by Common Receiver Gather (CRG), namely the set of traces generated by all the sources and recorded at the same receiver. Figure 1 illustrates this approach: if two adjacent receivers have a different near surface delay, it is common to all the traces of the same CRG. Then this delay could be detected by a delay measurement method such as crosscorrelation, applied to  $PS$ -wave reflections. In principle it could be assumed that the NMO effect (corresponding to  $M_k h_{ij}^2$ ) is negligible taking into account the short distance between the reflections.

The crosscorrelation between two traces is a tool to obtain the relative time delay between them (Taner et al., 1974; Li, 1999). Crosscorrelation measures the similarity between two time series after a delay, multiplying a series with a time shifted version of the other one, as follows:

$$C_{ab}(\tau) = \frac{\sum_t D_a(t) D_b(t + \tau)}{\sqrt{\sum_t D_a(t)^2 \sum_t D_b(t)^2}} \quad (2)$$

where  $D_a(t)$  and  $D_b(t)$  are the two traces,  $\tau$  is the shift time and  $C_{ab}(\tau)$  is the crosscorrelation for the time delay  $\tau$ . The divisor in equation 2 makes a normalized result, since the maximum possible value is 1 for the case when both traces are identical (Li, 1999).

Thus each traces of a CRG can be crosscorrelated with the trace of the adjacent CRG

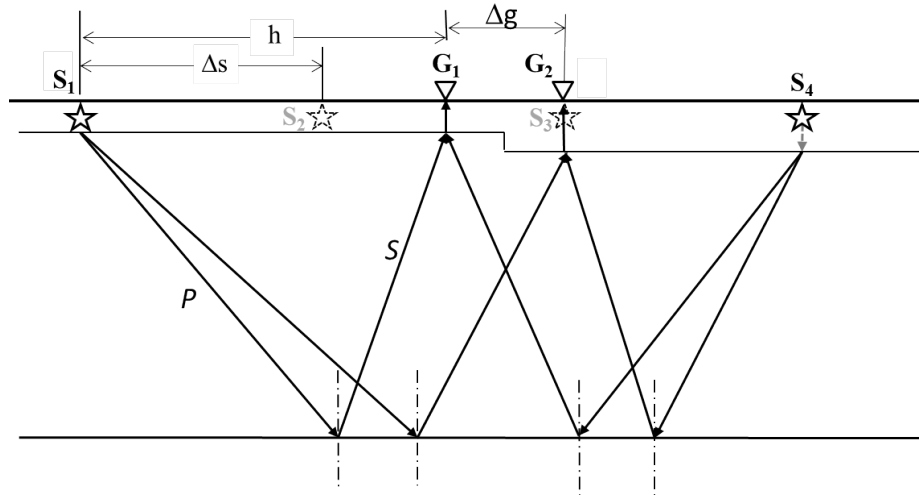


FIG. 1. The *PS* events used for crosscorrelation in the receiver statics algorithm illustrated by ray-paths. Each trace of a CRG is crosscorrelated with the trace of the adjacent CRG corresponding to the same source. Both CRGs are corrected for source statics. The relative time delay corresponds to the differential receiver time delay in the NS-LVL, plus the offset and geological time delays.

corresponding to the same source location, and the resulting crosscorrelations are added together. The method just described can be expressed by the next equation:

$$C_{ab}(\tau_k) = \sum_{j=1}^{N_h} \sum_{i=1}^{N_t} \frac{D_a(t_i, h_j) D_b(t_i + \tau_k, h_j)}{\sqrt{\sum_t D_a(t_i, h_j)^2 \sum_t D_b(t_i, h_j)^2}} \quad (3)$$

where  $D_a$  and  $D_b$  are corresponding traces of adjacent CRGs with  $N_h$  traces and  $N_t$  time samples, and  $\tau_k$  corresponds to the time shift between the two traces.

A data gate can contribute to carry out this analysis, since it allows to keep out strong coherent noise events, such as surface waves and first arrivals (shallow refractions), and to include *PS* wave reflected arrivals. The data gate should be as long as possible to allow redundancy in the cross-correlation. It is assumed that the horizontal component has enough *PS* wave energy, however selecting *S*-waves by wave mode separation methods could also contribute to better analysis.

### SYNTHETIC DATA TEST

A test of this method on a synthetic model is now described. The data was generated using a Finite Difference elastic modeling method (Levander, 1988). The model is roughly based on the real near surface environment presented in Guevara et al. (2013). Fig. 2 illustrates the *S*-wave velocity model and Fig. 3 the *P*-wave velocity. The  $x$  coordinate increases from left to right, and the  $z$  coordinate increase from top to bottom. The horizontal size is 1000 m and the vertical is 600 m. The surface is assumed to be flat and 75 m deep. Receivers are separated by 5 m and sources spaced at 20 m intervals. The geology at depth is quite simple, composed of horizontal layers, each one characterized by a velocity, which increases with depth. The NSL *P*-wave velocity is constant. The NS layer has a gradual increase in the *S*-wave velocity with depth, from about 100 m/s at the surface to a velocity close to the consolidated rock. Five lateral zones were established for  $V_S$ , each one

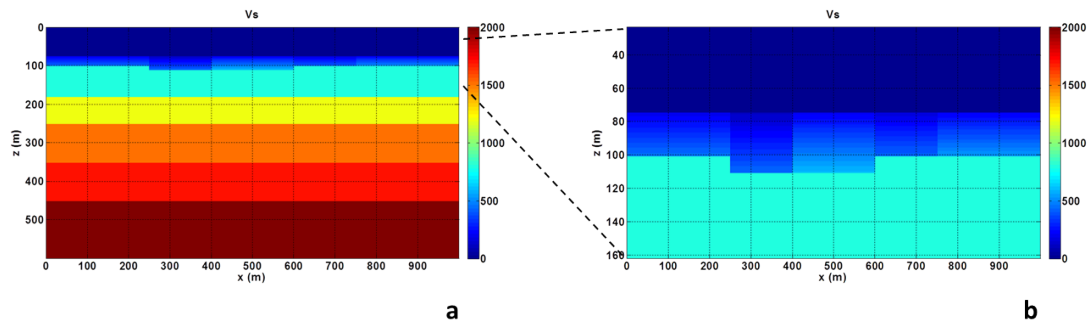


FIG. 2.  $S$ -wave velocity model to test the  $PS$  receiver statics algorithm. (a) Layers distribution. The free surface, where sources and receivers are located, is at a depth of 75 m. After that is the LVL and five more consolidated rock layers with flat interfaces. (b) Closeup of the NS Layer. Notice the gradual increase in velocity with depth and the lateral velocity discontinuities.

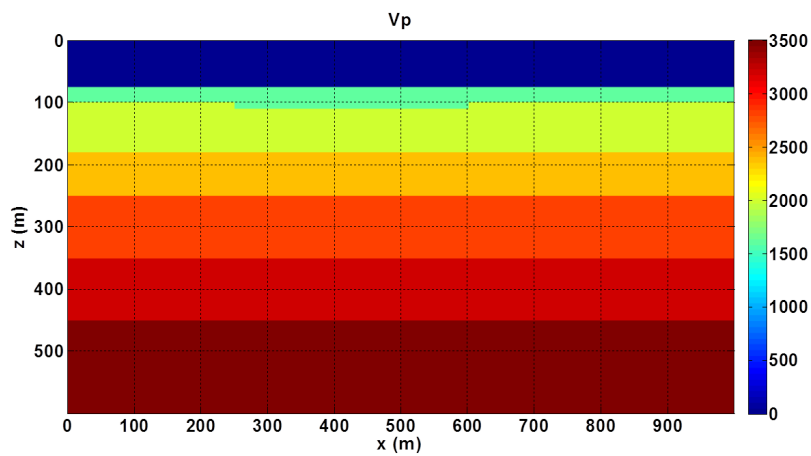


FIG. 3.  $P$ -wave velocity model to test the  $PS$  receiver statics algorithm. The free surface is at a depth of 75 m, below which there is a LVL and five more consolidated rock layers with flat interfaces. The NSL velocity is constant and close to the underlying layer velocity.

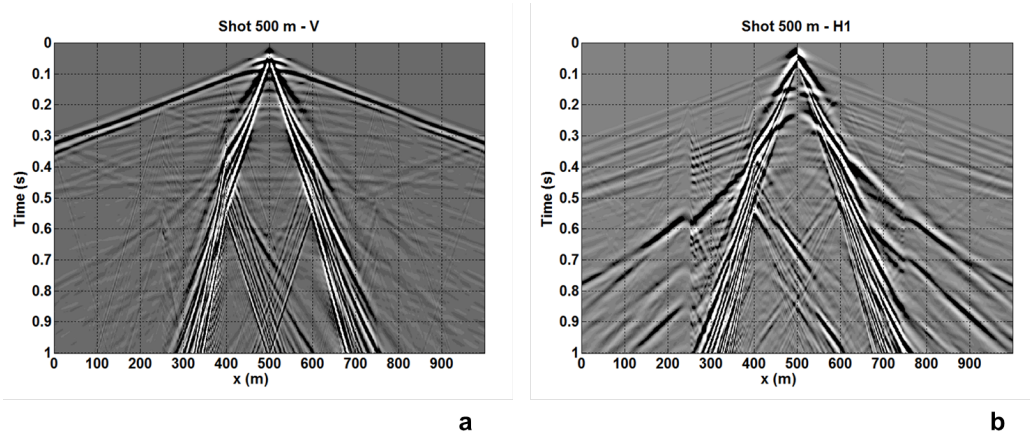


FIG. 4. Shot gathers for vertical and horizontal components of the synthetic data test for the *PS* receiver statics method. (a) Vertical component, (b) Horizontal component. Notice the weak first arrivals in (b), and the strong events that resemble the horizontal NSL *S*-wave velocity variation. It includes *PS* reflections and probably *S* wave refractions.

Receiver location	$V_S$	Time ( $20/V_S$ )	Time differential (s)
245	340	0.059	0.019
255	255	0.078	
395	255	0.078	-0.025
405	380	0.053	
595	380	0.053	0.009
605	315	0.063	
745	315	0.063	-0.012
755	393	0.051	

Table 1. Time delays calculated from the synthetic model 1. Theoretical time delay at the surface locations where the NSL changes its properties.

with a different NS *S*-wave velocity and with thicknesses between 25 and 35 m, as shown in the close-up of figure 2 (b).

As examples of the seismic modeling output, figure 4 shows records of the two components of a shot, located at the surface coordinate  $x=600\text{m}$ . The vertical component is shown in figure 4 (a) and the horizontal radial component in figure 4 (b). The vertical component shows *P*-waves and the horizontal component mostly *S*-waves, as expected according to the polarization of each wave mode. Notice lateral variations of the events in the horizontal component (*S*-waves), which correspond to the lateral variation of the near surface velocity (figure 2).

Theoretical differential delay times were calculated from the average velocity for each lateral variation of  $V_S$  in the NSL, assuming a mean thickness of 20 m. The values used for calculation are in the three left hand side columns of Table 1, and the differential delays are in last column. These differential delays can be compared with the results analyzed in the following sections.

The method just described was applied to the modeling data crosscorrelating traces

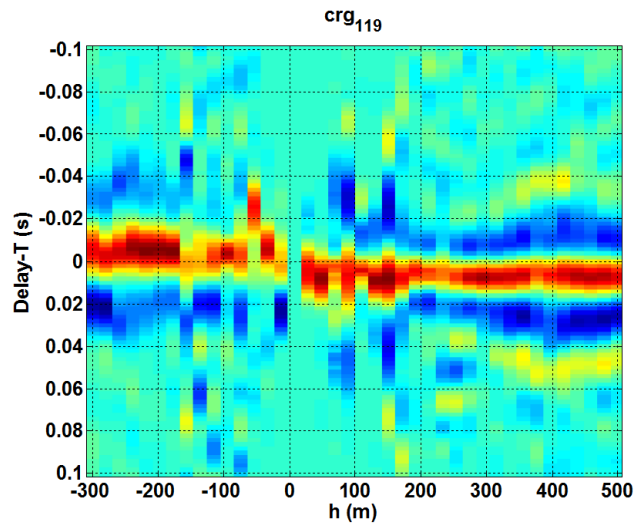


FIG. 5. Results of crosscorrelation of common receiver gathers for adjacent receivers about  $x=600$  m. Notice a difference in time delay between positive offsets and negative offsets, which can be explained by the differential NMO (Fig.1).

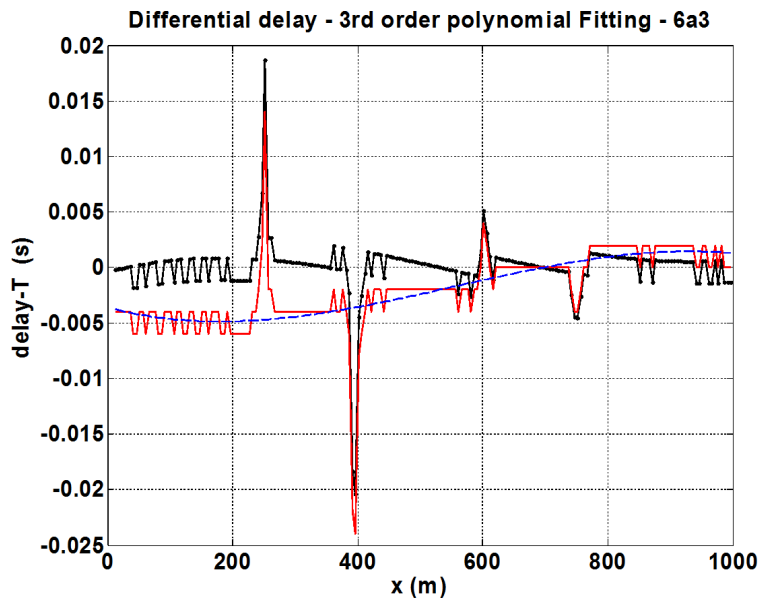


FIG. 6. Picking of maximum results of crosscorrelation of common receiver gathers. The red line corresponds to the raw picking, the blue line to the low frequency component, and the black line to the picking corrected after subtraction of the low frequency component.

of adjacent receiver gathers that correspond to the same source. An example of these crosscorrelations is in Fig. 5 corresponding to the receiver located close to  $x = 600$ . Then these crosscorrelations are stacked and only one value is obtained for each couple of CRGs. After that the delay time corresponding to maximum of the stacked crosscorrelation is extracted and all the delay times are plotted. This result is illustrated in Fig. 6 by the red line. It can be compared to Table 1, that has differential statics at locations  $x=250, 400, 600$  and  $750$ . The most noticeable events are at the same locations in Fig. 6, which agrees with the hypothesis. However there is a low frequency trend, such that the left hand side delay times are negative and the right hand side events are positive.

After this test it was shown that there is a meaningful error in the delay times generated by the difference in offset between traces of adjacent receiver and the same source. It is illustrated by figure 1. This misfit has a noticeable effect on the resulting statics analysis. An option to overcome this issue would be to have the same offset for the two traces to be crosscorrelated. Since offset depends on the distance between sources and receivers, it would be possible to obtain the same offset in the traces to be crosscorrelated by interpolating near traces. A test using this idea is presented in the following section.

#### *Compensating for the NMO time delay*

The Radon transform have been used for data interpolation, e.g. Kabir and Verschuur (1995). A version of the Radon Transform used in geophysics, known as the  $\tau - p$  transform was used in this case. The  $\tau - p$  transform or *slant-stack* transfer the seismic data from the *time-space* coordinates ( $t - x$ ) to the intercept time ( $\tau$ ) -ray parameter ( $p$ ) domain, according to the equation:

$$u(\tau, p) = \int_{-\infty}^{\infty} u(\tau + px, x) dx \quad (4)$$

The ray parameter is defined as the *horizontal slowness*, that is to say

$$p = \frac{\sin\theta}{v} \quad (5)$$

where  $\theta$  is the angle of incidence and  $v$  is the velocity of the incident wave.

It is a plane wave decomposition of the wavefield, where the ray parameter corresponds to a plane wave component. The  $\tau - p$  transform is reversable, then it is possible to get back the  $t - x$  domain data, after some convenient operation in the  $\tau - p$  domain. In this case this operation is a resampling of the CRG data in the  $x$  domain, such that the new resampling agrees with the offsets of the corresponding adjacent CRG.

In order to calculate the time delay between two receivers, say 1 and 2, a trace from receiver 1 is cross-correlated with the corresponding interpolated trace with the same offset from receiver 2. Subsequently, the original, non-interpolated trace from receiver 2 is cross-correlated with the corresponding interpolated trace that has the same offset from receiver 1. Traces 1 and 2 may correspond to reflections from different depths, but these differences due to geological structure should be attenuated when the average results is used. Possible

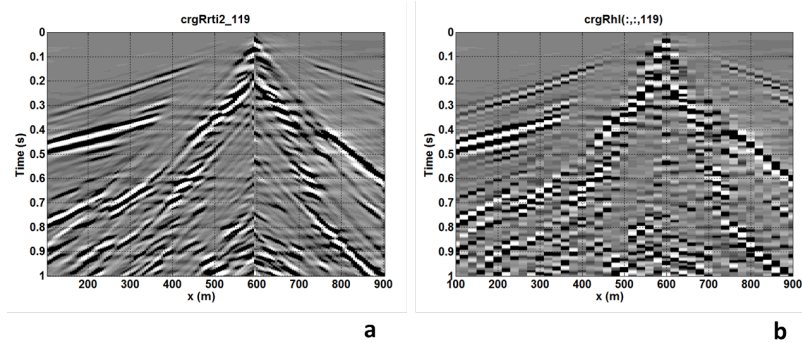


FIG. 7. Interpolation of the CRG from the acquisition offsets to the offsets of the adjacent CRG. (a) Interpolation from the distance between sources (20 m) to the distance between receivers (5 m), (b) resampling to the offsets of the adjacent CRG .

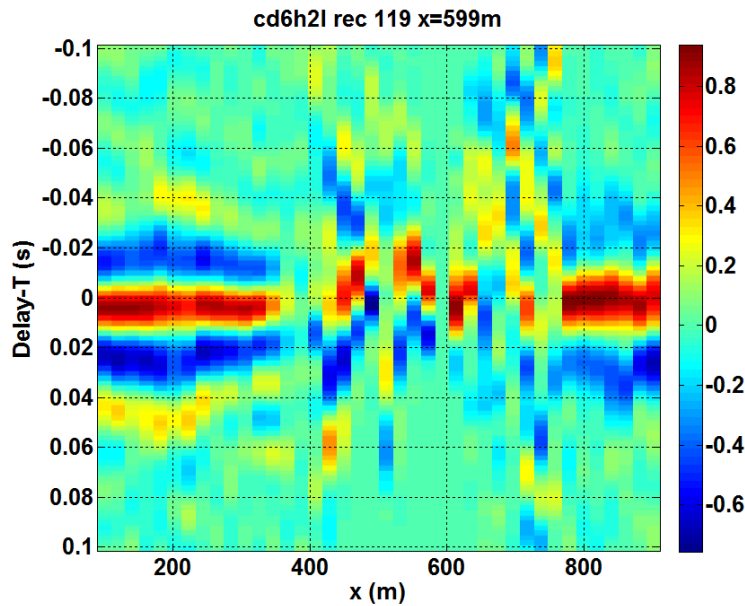


FIG. 8. Crosscorrelation of CRGs at  $x=599\text{m}$  after interpolation, then both CRGs have the same offset. It can be noticed that there is a small difference in the crosscorrelation picks between positive and negative offsets. The short offsets (between  $x=400$  to  $x=750$ ) crosscorrelation is poor.

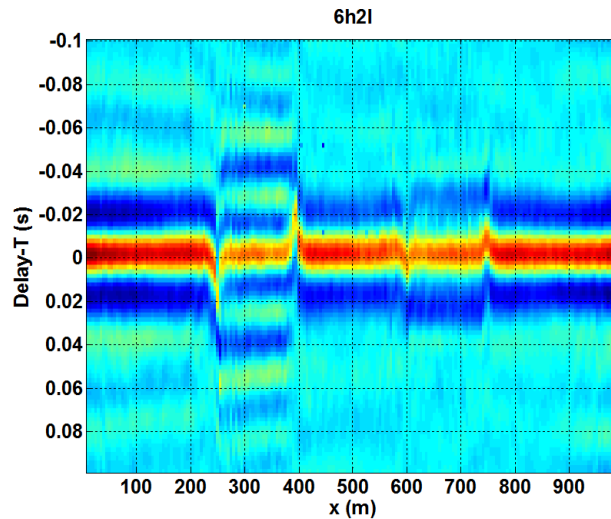


FIG. 9. Summation of pairwise crosscorrelations of adjacent CRGs from left to right. Each trace of a CRG is crosscorrelated to the corresponding offset trace after interpolation of the adjacent CRG towards larger  $x$  coordinate.

errors resulting from the interpolation should also be attenuated, given that in each case interpolation is done on a different CRG.

The method is applied to the same synthetic dataset. In this dataset sources are located at receiver locations, separated by a distance four times the distance between each receiver. The CRG traces are interpolated to obtain all the intermediate values, as if there were sources at each receiver location. Figure 7 shows a data set interpolated corresponding to the CRG at  $x=599$  Figure 7 (a) corresponds to the complete interpolated CRG, from which it was extracted the dataset of figure 7 (b), that corresponds to the offsets of the adjacent CRG to its left hand side (toward lower  $x$ -values in figure 2).

After application of trace interpolation to obtain traces with the same offset distance (Fig. 8), there is no difference in the trend of the data between offset values of opposite sign (corresponding to high  $x$  values for the negative offsets and low  $x$  values for the positive offsets). This, however, was not the case when interpolation was not carried out, where traces with offset differences of about 5 m were being cross-correlated (Fig. 5). One can also observe peaks in the cross-correlation which are related to the lateral velocity variations of the low-velocity model. The result is of opposite sign if the cross-correlation is performed from left to right.

Figure 9 shows the crosscorrelation results for all the CRGs when the analysis is carried out forward (from lower to higher  $x$ ), and figure 10 shows the analogous correlation results when the analysis is carried out backwards (from higher to lower  $x$ ).

The maximum values of both crosscorrelation analyses are presented in figure 11, The blue continuous line with dots corresponds to the forward calculation and the red dashed line with stars to the backward calculation. It shows the opposite polarity for each method at the NS  $V_S$  variation locations. An additional delay of 2 ms for all the CRGs in both methods can be also noticed. This delay can be explained as a phase effect of the interpolation

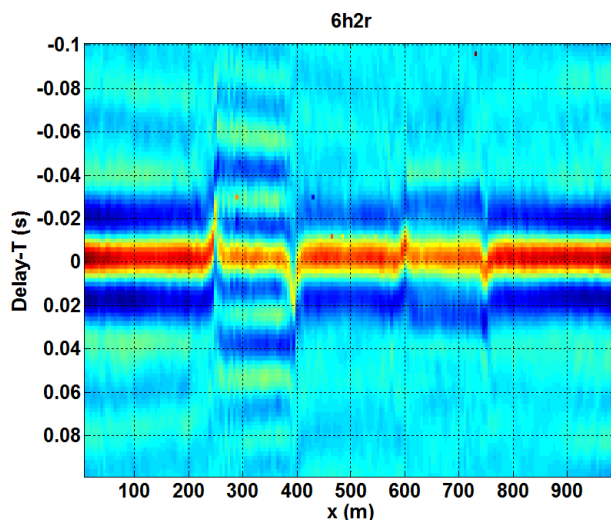


FIG. 10. Summation of pairwise crosscorrelations of adjacent CRGs from right to left. Each trace of a CRG is crosscorrelated to the corresponding offset trace after interpolation of the adjacent CRG towards smaller  $x$  coordinate.

using the  $\tau - p$  transform. It also suggest a method to overcome this delay: subtracting the backward calculation from the forward calculation and halving the result, the value of zero can be recovered and the time delay due to the variation in the NS  $V_S$  variations are obtained. The result of this operation is observed in figure 12.

These values are assumed as the differential receiver statics, and the statics correction is obtained from them, by addition through the CRG locations in the forward direction. The resulting statics is shown in figure 13, corresponding to the blue line. The theoretical statics calculated from data of the table 1 is also represented by the red dashed line as for comparison. Although the trend is broadly similar, we notice the remarkable effect that small anomalies in the value of the integral. It can be noticed that the delay time is not limited to a point but extends to two or three adjacent receivers. This could be explained by the limitation of the hypothesis of consistency in surface and the nature of the wavefront, not restricted to a ray as assumed.

#### *A method to obtain a single differential and the statics correction*

As shown by Figs. 11 and 12 differential statics is extended beyond the change in velocity, which generate an accumulative effect in integration such that static correction can be distorted. A test to attenuate this effect was carried out and is presented in the following figures. The first step was to select only the picks, such that the delay is limited to a few locations and the second step was to define a threshold, assuming that the delays smaller than 4 ms are not reliable. Fig. 14 shows the differential delay resulting of these steps. Fig. 15 shows the static delay after integration of the previous differentials. Finally Fig. 16 shows the shot gather corresponding to the location  $x=900$  m, before statics application in Fig. 16 (a) and after statics application in Fig. 16 (b). Notice that there is an improvement in the continuity of the events, e.g. offsets between -500 and -650 m.

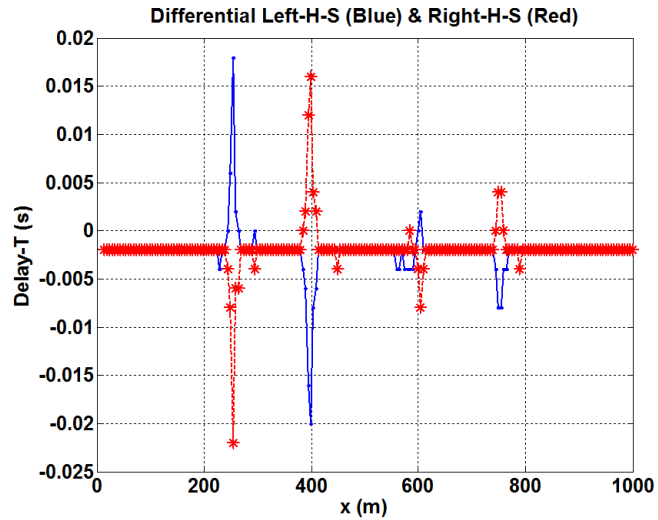


FIG. 11. Picking of the maximum CRG crosscorrelations in both directions. The dashed red line with asterisks corresponds to the right-hand-side crosscorrelation, and the blue continuous line with dots to the left-hand-side crosscorrelation. Both have opposite polarity at the lateral NS  $V_s$  variations and a common constant delay of 2 ms.

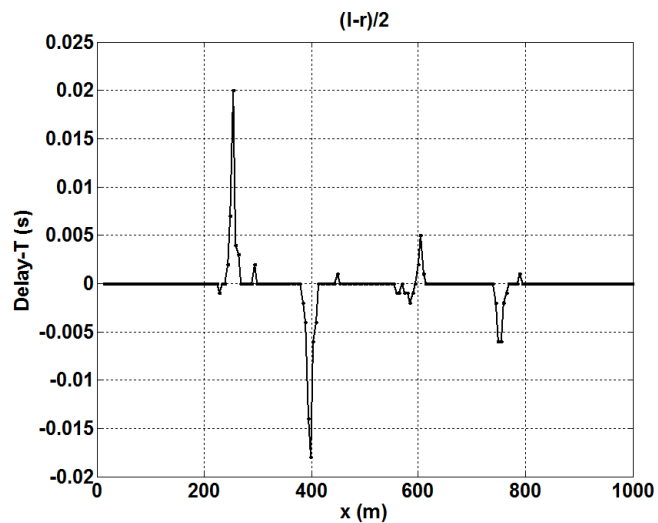


FIG. 12. Summation of the maximum CRG crosscorrelations in both directions. The right-hand-side crosscorrelation maximum was subtracted from the maximum left-hand-side and the result divided by two. It can be noticed that the two ms constant delay was eliminated.

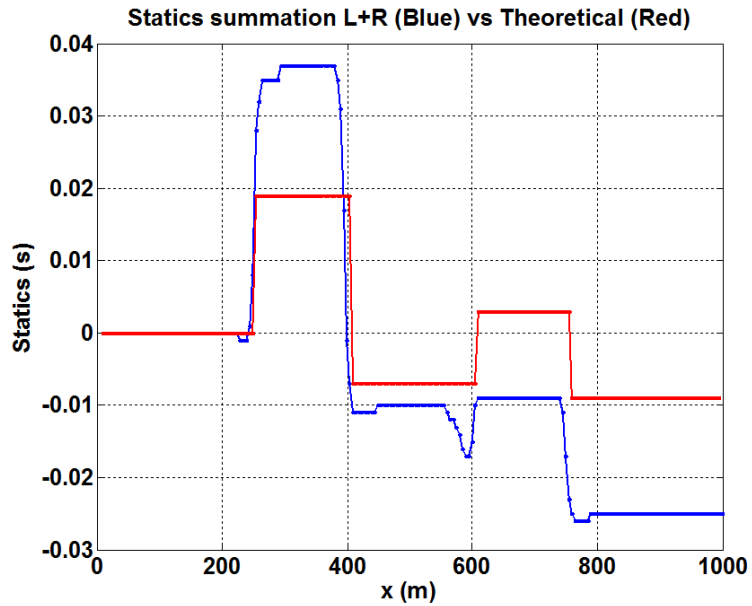


FIG. 13. Statics calculation after interpolation (blue line), obtained by summation on the  $x$  direction, compared with theoretical (red line).

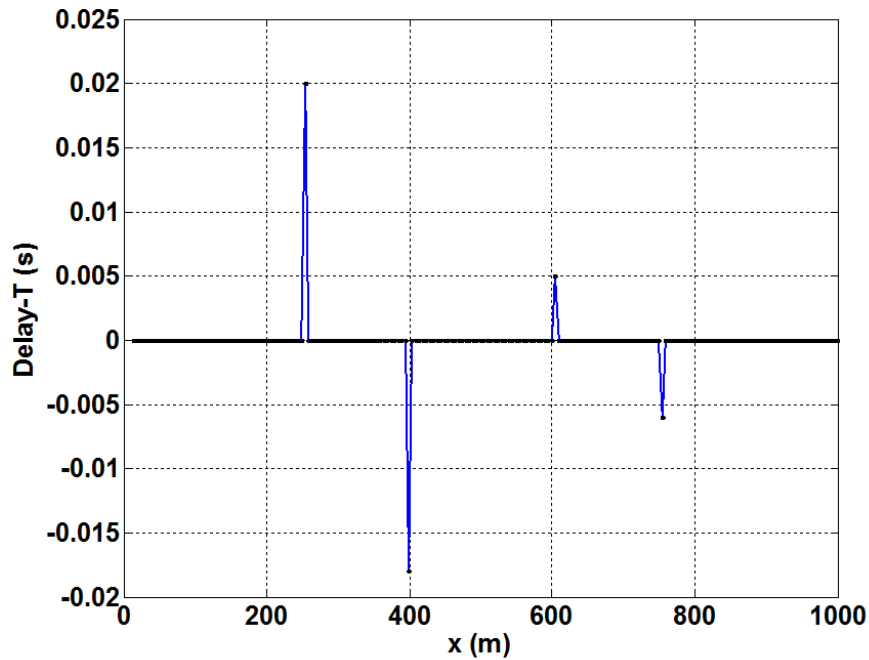


FIG. 14. Differential delay time after filtering. Filtering had two steps: getting the isolated pick and defining a threshold to eliminate delays shorter than 4 ms.

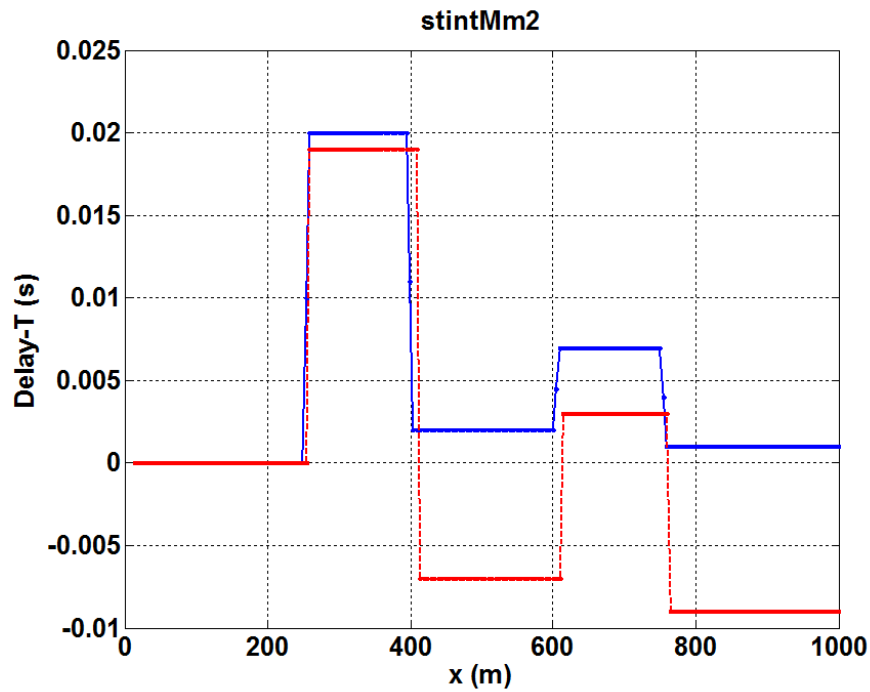


FIG. 15. Statics calculation after interpolation and filtering to obtain the differential statics of Fig. 14 (blue line), obtained by summation on the  $x$  direction, compared with the theoretical (red line).

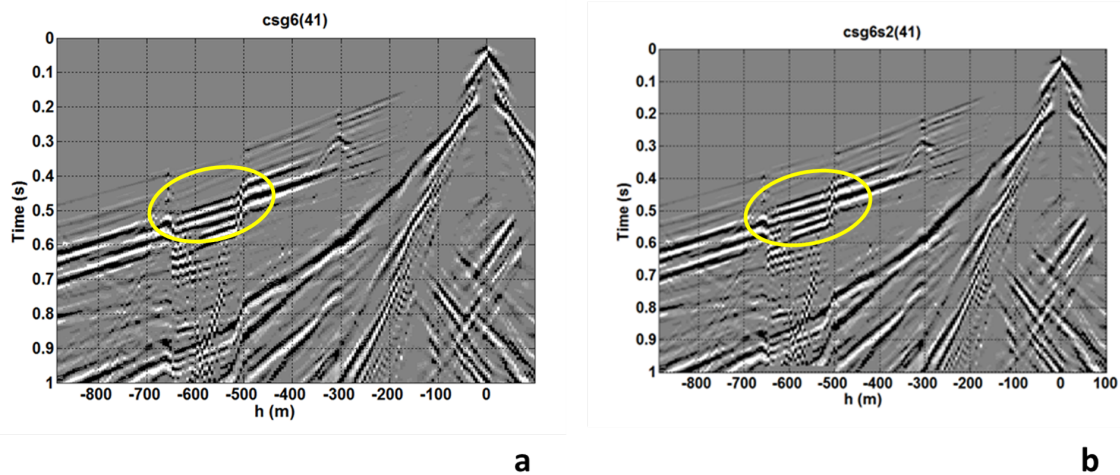


FIG. 16. Effect of the receiver statics correction on the CSG with the source located at  $x=900$  m. (a) before and (b) after receiver statics correction.

## DISCUSSION

The previous results confirm the working assumptions, namely that there are *S*-waves in the prestack data, which show meaningful information about the receiver static time delay, using the surface consistent model. The receiver statics differential delay time can be estimated by crosscorrelations (compare Table 1 and Fig. 14), without stacking of the *PS*-wave events. The experiments carried out to extract statics from these data suggest some issues that worth considering.

As noticed by Cox (1999), there are a number of possible sources of error in the statics correction using the surface consistent approach, namely the moveout effect, the geologic structure or dip, possibility of cycle skipping in picking, and remaining noise contamination.

In fact, there is a moveout differential due to the difference in offset between the two traces to be cross-correlated, as illustrated in Fig. 1. It has a meaningful effect as shown by the difference between the negative and positive offset crosscorrelations of a CRG in Fig. 5 and the low frequency component in the maximum crosscorrelations picked in Fig. 6. However it is possible to get traces at the same offset by interpolation of the traces inside a CRG. After that, a relatively simple interpolation method was used, and the offset effect appears greatly overcome as can be noticed comparing Fig. 6 and Fig. 12, which supports this approach.

Regarding the geologic structure, a minor time delay component can be expected, because of the short distance between receivers and taking into account that it is not systematic (could be assumed random) in the receiver domain, whose crosscorrelations will be stacked. The interpolation can also contribute to its attenuation. As for the possible cycle skipping, it is least feasible if the number of seismic events is greater, so it can depend on the gate selected. In the case of noise contamination, coherent noise events such as surface waves can be quite strong compared with *PS*-waves, then amplitude corrections and again an appropriate analysis gate are advisable.

On the other hand, the method proposed assumes vertical time delay (statics) and surface consistency, which is an approximation. It can be noticed that the delay time is not limited to a point but extends to two or three adjacent receivers (e.g. Fig. 12). This could be explained by the limitations of these hypotheses, and the nature of the wavefront.

## SUMMARY AND CONCLUSIONS

1. A method for receiver statics correction of *PS*-waves is proposed here, which is based on the surface consistent model applied to Common Receiver Gathers (CRG), a surface domain. It requires prestack traces which are crosscorrelated between adjacent CRG to get the differential statics between them. Thus,  $V_c$  (stacking velocity for converted wave) is not required.
2. The traces should be corrected by source statics, and interpolation appears as a method to compensate for the delay time caused by the offset differential (NMO). Filtering of high energy noise and amplitude correction appear also convenient.

3. The method was tested on a synthetic model of elastic waves, showing promising results. Trace interpolation and filtering of the resulting delay times contributed to a reasonable resulting statics.
4. The method proposed can provide the short wavelength component of the statics solution. It can make the statics correction and the velocity analysis conveniently separated in the processing of *PS*-wave.
5. If there were shallow borehole information available, the resulting statics model could contribute to improve the velocity model shallower than 15 m depth.
6. The statics model and the surface consistency can be subject of further tests, including real data and geological structure.

### ACKNOWLEDGEMENTS

We thank the sponsors of CREWES who supported this research. We also gratefully acknowledge support from NSERC (Natural Science and Engineering Research Council of Canada) through the grant CRDPJ 379744-08. CREWES staff contributed greatly. Special recognition to Rolf Maier and Kevin Hall for their computing support.

### REFERENCES

- AIDulaijan, K., 2008, Near-surface characterization using seismic refraction and surface-wave methods: M.Sc. thesis, Univ. of Calgary.
- Cary, P. W., and Eaton, D. W., 1992, A simple method for resolving large converted-wave P-SV statics: *Geophysics*, **58**, No. 3, 429–433.
- Cox, M., 1999, Static corrections of seismic reflection surveys: SEG Geophysical Reference Series, Tulsa, OK, USA.
- Disher, D. A., and Naquin, P. J., 1970, Statistical automatic statics analysis: *Geophysics*, **35**, No. 4, 574–585.
- Guevara, S. E., Margrave, G. F., and Agudelo, W. M., 2013, Near surface S-wave velocity from an uphole experiment using explosive sources: 83th Ann. Internat. Mtg., Soc. Expl. Geophys. Expanded Abstracts, 1694–1698.
- Harrison, M. P., 1992, Processing of PSV surface-seismic data: anisotropy analysis, dip moveout and migration: Ph.D. thesis, Univ. of Calgary.
- Kabir, M. M. N., and Verschuur, D. J., 1995, Restoration of missing offsets by parabolic radon transform: *Geophysical Prospecting*, **43**, No. 3, 347–368.
- Levander, A. R., 1988, Fourth-order finite-difference P-SV seismograms: *Geophysics*, **53**, No. 4, 1425–1435.
- Li, X. X., 1999, Residual statics analysis using prestack equivalent offset migration: M.Sc. thesis, Univ. of Calgary.
- Schafer, A. W., 1993, Binning, static correction, and interpretation of P-SV surface-seismic data: M.Sc. thesis, Univ. of Calgary.
- Taner, M. T., Koehler, F., and Alhilali, K. A., 1974, Estimation and correction of near-surface time anomalies: *Geophysics*, **39**, No. 4, 441–463.